

Plasma Electron Density Measurement Around Hypersonic Flight Experiment Vehicle

Takeshi Ito* and Ryoji Takaki†

National Aerospace Laboratory, Tokyo 182-8522, Japan
and

Ken Teraoka‡

National Space Development Agency, Tokyo 182-8522, Japan

The hypersonic flight experiment (HYFLEX) vehicle, which was a joint project for a hypersonic flight experiment between the National Aerospace Laboratory and the National Space Development Agency of Japan, was successfully launched from the Tanegashima Space Center by a J-1 rocket on 12 February 1996. The plasma electron density at the windward surface of the HYFLEX vehicle was measured using reflectometers, which are nonintrusive measurement devices. The reflectometer employs a phenomenon in which the radio waves are reflected from the plasma layer when the plasma density increases and exceeds a certain value. For comparison, the plasma density could also be calculated from a numerical analysis by real-gas computational fluid dynamics. It was difficult, however, to verify a real-gas computational fluid dynamics code using ground facilities. Here the flight data were compared with the calculations using a numerical simulation of the interaction between the radio waves and calculated plasma electron density. Also, this technique was applied to a prediction of the intensity of telemetry received at the Ogasawara Downrange Station during the flight of HYFLEX. These simulations agreed well with respect to the intensity of reflected and received radio waves, which is related to the plasma electron density measured during the flight. However, an interesting discrepancy remained in the timing of the reflection peak and blackout occurrence.

Nomenclature

B	= magnetic field
c	= speed of light
E	= electric field
e	= charge of electrons
f_p	= plasma frequency
J	= current density
m	= mass of electrons
n_p	= number density of plasma electrons
t	= time
v	= velocity of electrons
x	= location of electrons

Introduction

AS a part of a program to develop a reusable space transportation system for Japan, the development phase of its full-scale demonstrator, the H-II Orbiting Plane-Experiment (HOPE-X), has started its last fiscal year and is in design phase C as a joint project between the National Aerospace Laboratory (NAL) and the National Space Development Agency of Japan (NASDA). The flight of HOPE-X is slated for around 2003, according to the present official schedule. Prior to the start of HOPE-X development, a series of flight experiments using smaller vehicles [for the orbital reentry experiment (OREX), for the automatic landing flight experiment (ALFLEX), and for the hypersonic flight experiment (HYFLEX)] was planned to demonstrate the key technologies necessary for HOPE-X.^{1,2}

Among these flight experiments, HYFLEX was successfully conducted on 12 February 1996. The vehicle was launched from the Tanegashima Space Center by the J-1, which is a new solid rocket developed by NASDA. The purposes of the HYFLEX project are to acquire experience from the design, manufacture, and flight of a hypersonic lifting vehicle. Moreover, flight data on aerodynamics and aerothermodynamics, performance of the thermal protection system, guidance and control, and blackout phenomena are obtained for the evaluation of design and test tools on the ground. Also, hypersonic flight experiment technologies will be improved.^{3–9}

The flight plan is shown in Fig. 1. The planned maximum velocity of the HYFLEX was about 3.9 km/s. It was predicted that the vehicle would encounter maximum aerodynamic heating at an altitude of about 45 km and at a flight Mach number of about 11 at 49-deg angle of attack. The planned flight time from separation to Mach 2 (end of attitude control) was 341 s.

In this paper, we focus on reflectometer measurement results among the acquired flight test results, which are related to the ionization of the air state around the vehicle. When spacecraft such as Apollo and the Space Shuttle reentered the Earth's atmosphere, blackout phenomena occurred. Blackout is the phenomenon in which radio waves are reflected from ionized air around the airframe at hypersonic flight. Although radio wave blackout is no longer a problem in reentry flight because of high-frequency communication via data relay satellites, the real-gas effect, which is caused by dissociation and ionization of the air around the airframe, is considered to be the cause of the aerodynamic characteristics deviating from those predicted during the first flight of the Space Shuttle and are not negligible.^{10,11}

The plasma electron density at the windward surface of the HYFLEX vehicle was measured using reflectometers, which are nonintrusive measurement devices. Reflectometers employ a phenomenon in which the radio waves are reflected by the plasma layer when the plasma density is higher than a certain value. Thus, plasma electron density can be evaluated from the reflection intensity of the radio waves. Also, the intensity of very-high-frequency (vhf) telemetry signals received at the Ogasawara Downrange Station was measured. Power loss of this telemetry was also caused by radio wave cutoff through the plasma layer around the vehicle, so that the change in intensity could be used for comparison with the data from the reflectometer.

Presented as Paper 98-2480 at the AIAA 29th Plasmadynamics and Lasers Conference, Albuquerque, NM, 15–18 June 1998; received 6 July 1998; revision received 17 November 1998; accepted for publication 18 November 1998. Copyright © 1999 by the American Institute of Aeronautics and Astronautics, Inc. All rights reserved.

*Senior Researcher, Fluid Science Research Center, 7-44-1 Jindaiji-Higashi, Chofu. Member AIAA.

†Researcher, Computational Science Division, 7-44-1 Jindaiji-Higashi, Chofu. Member AIAA.

‡Engineer, HOPE-X Project Team, Office of Space Transportation Systems, c/o National Aerospace Laboratory, 7-44-1 Jindaiji-Higashi, Chofu.

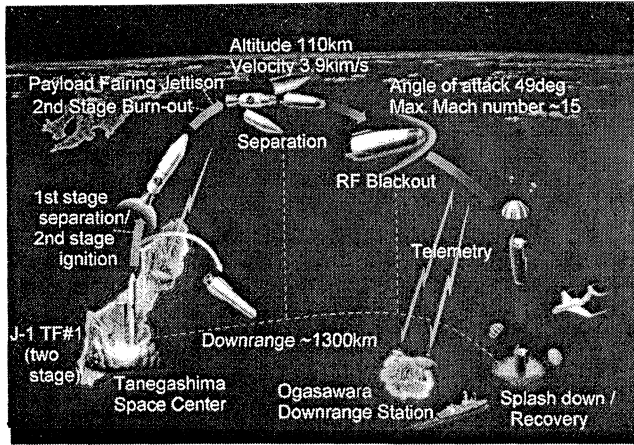


Fig. 1 Flight plan of the HYFLEX.

For comparison and code validation, the plasma density can be calculated from a numerical analysis by real-gas computational fluid dynamics (CFD) codes. It is difficult to verify real-gas CFD codes using ground facilities because of various limitations such as flow conditions, size of the model, instrumentation, and so on. Also, flight data concerning real gas effects are scarce, even though there are some indirect flight data such as heat transfer rates and aerodynamic influences. Therefore, HYFLEX is a very promising chance for validation. Here the reflection intensity for the reflectometers and the received intensity at the downrange station during the flight were compared with the calculations using numerical simulation of the interference between radio waves and the CFD-calculated plasma electron density.

Example of CFD Predictions Including Real-Gas Effects

To design the reflectometers before manufacture, real-gas CFD analysis is one of the most useful techniques for producing some simulation data of the plasma density and distribution around the vehicle. Although the CFD simulation needs to be verified by flight data, it is adequate to use for designing this type of measurement system.

The plasma electron density around the HYFLEX vehicle during its atmospheric flight could be predicted by the CFD code in Refs. 12–14, which included the real-gas effects (numerical calculation of the flowfield including dissociation and recombination of the gas). The calculated flowfield was a three-dimensional, steady-state, viscous flow of mixed chemical species (O_2 , N_2 , N , O , NO , NO^+ , and e^-). Finite-rate chemical reactions and Park's two-temperature model, which had two internal energy modes (translational and rotational energy mode and vibrational and electron excitation energy mode) were considered to take into account nonequilibrium effects. Millikan and White's semi-empirical equation with Park's modification of limiting collisions of particles at high temperature (above 8000 K) was used as a relaxation model between vibrational temperature and translational temperature. The governing equations were the three-dimensional Navier–Stokes equations, mass conservation equations for each chemical species, and a conservation equation of the vibrational energy. Details of the CFD code are given in Refs. 12–14.

Figure 2 shows the calculated results of plasma electron density distribution along the center axis of the reflectometer antenna. The layer with the highest density is at the wall surface. The largest density occurs at $t = 120$ s at the wall and is about 10^{11} (particles/cm³). Here the thickness of the plasma layer is very thin compared to the wave length (20–30 cm). The increase in density near the wall was caused by the noncatalytic condition. Although there are some results using a catalytic wall condition,^{14,15} it is difficult to find adequate catalytics for this type of ceramic tile surface. Therefore, we consider the results using a noncatalytic condition in the simulation.

The CFD results for the simulation of the vhf blackout (Fig. 3) show the plasma electron density distribution near the vhf telemetry antenna in the direction toward the Ogasawara Downrange Station.

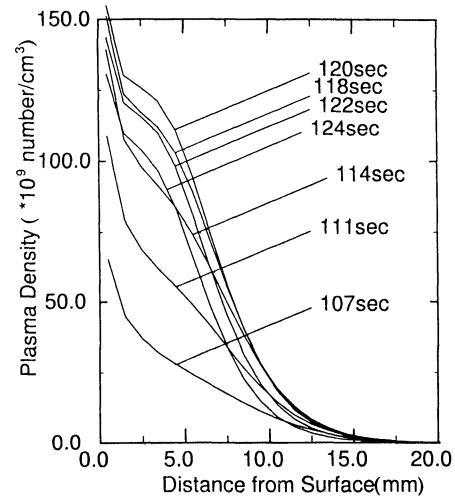


Fig. 2 Plasma electron density distribution calculated by CFD including real-gas effects: along the center axis of the reflectometer antenna.¹²

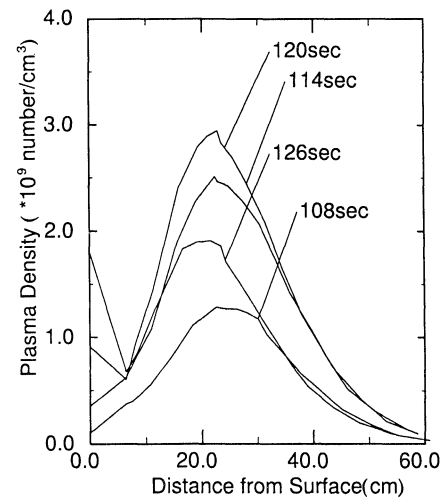


Fig. 3 Plasma electron density distribution calculated by CFD including real-gas effects: around the vhf telemetry antenna toward the Ogasawara Downrange Station.¹²

The peak of the plasma electron density occurs at a position 20 cm from the antenna, and the maximum density is about 3×10^9 (particles/cm³). The difference between the results of Figs. 2 and 3 is from the vhf antenna being located at a leeward surface of the HYFLEX vehicle. In other words, the aerodynamic heating at the leeward surface is not as high as at the windward surface, and there is a large separation region at the leeward area.

Measurement Principle Using Radio Wave Cutoff and Design of the Reflectometer

For the measurement of the plasma electron density around the vehicle, we adopted a reflectometer, which uses the cutoff phenomena of radio waves by plasma electrons. A radio wave cannot pass through a plasma layer when its frequency is lower than the plasma frequency, $f_p = (4\pi n_p e^2 / m)^{0.5} / 2\pi = 8970 \sqrt{n_p}$, which is determined by the free-electron number density n_p (particles/cm³), as shown in Fig. 4. This phenomenon is called radio wave cutoff by plasma electrons. Actually, the cutoff does not occur instantly. The reflection intensity from the plasma electrons increases gradually along with the increase of electron number density. The reflectometer is a system to measure the intensity of reflection normalized by the transmitted wave (the reflection coefficient) to determine the plasma electron density using the cutoff of radio waves.

Thus, it is important to choose a reflectometer radio wave frequency so that reflection from the plasma layer can occur. In the case of the HYFLEX during its development phase, it was predicted that the maximum number density n_p of plasma electrons would be on

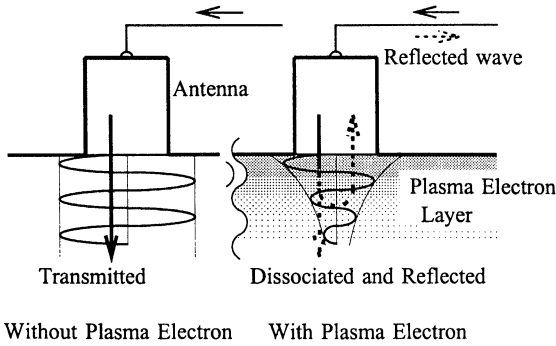


Fig. 4 Radio wave cutoff phenomena by the plasma layer.

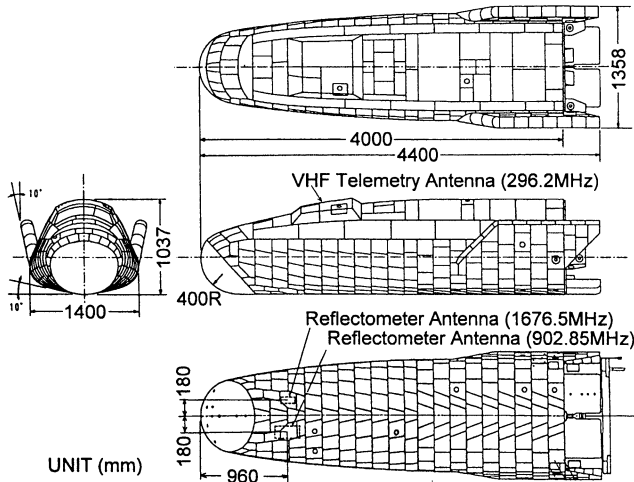


Fig. 5 Antenna locations of the reflectometer and vhf telemetry on the HYFLEX.

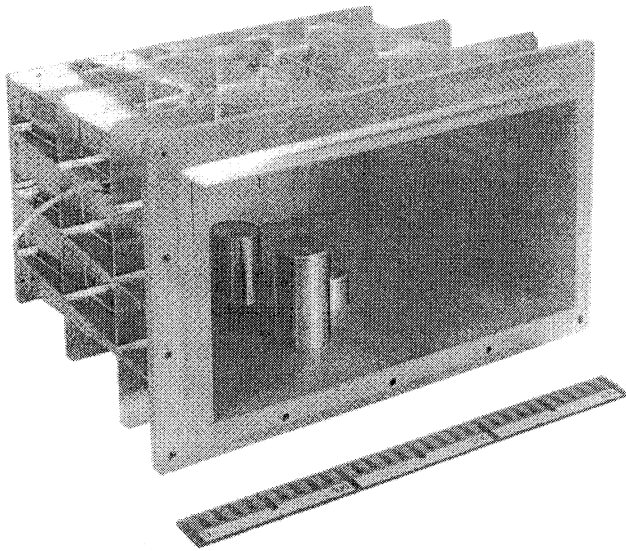


Fig. 6 Reflectometer antenna of 902.85 MHz.

the order of $10^{11}/\text{cm}^3$ and that the corresponding plasma frequency f_p would be about 3 GHz. Therefore, it was appropriate to set the frequency at 1 GHz or less because the reflection might decrease due to the plasma layer being thinner than the wave length. It is desirable to use more than one frequency to obtain the cutoff timing for different frequencies, i.e., the timing of different electron number densities, and so 902.85 and 1676.5 MHz were selected for the HYFLEX.

The antennas were installed 960 mm from the nose just aft of the carbon/carbon nose cap, and they were set 180 mm off the centerline (Fig. 5). This position was chosen to investigate the higher plasma density. The antenna was a rectangular waveguide type. The size of the opening of the 902.85-MHz antenna (Fig. 6) is 135×267 mm, and it is 74×145 mm for the 1676.5-MHz antenna. To allow the radio waves to be transmitted from the vehicle, a Kevlar® panel win-

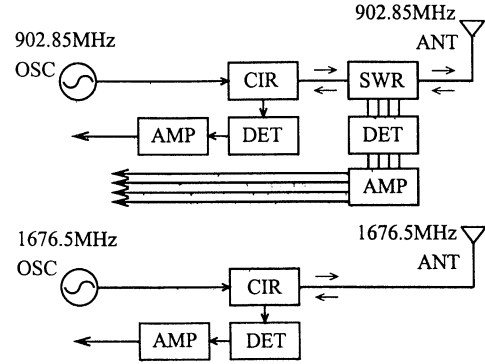


Fig. 7 Reflectometer circuit on the HYFLEX.

dow replaced the aluminum skin and the thermal protection tile was then attached to the outside of the panel. The electromagnetic effect of the panel and tile on the radio waves is negligible. Because of the distance between the plasma layer and the antenna, there is some influence on the reflection coefficient that the reflection simulations should consider.

The measuring system circuit is composed of an oscillator, circulator, standing wave ratio (SWR) section (for 902.85 MHz only), detector, and amplifier (as shown in Fig. 7). The radio wave is transmitted from the oscillator to the antenna through the circulator and then reflected from the plasma layer. The reflected wave enters the detector from the antenna by the circulator and finally is received by the detector, where the intensity of the reflected wave is measured. In the SWR section, the phase of the reflected wave is measured by detecting the standing wave when full reflection of the radio waves occurs. This gives information on the distance from the antenna to the plasma layer. Unfortunately, the accuracy was so bad that we cannot discuss the flight data.

Additionally, telemetry data were received normally at the Ogasawara Downrange Station except during the blackout.¹⁶ The blackout was observed in vhf telemetry (296.2 MHz) between 105 and 125 s from separation. (Flight data during the blackout were stored onboard and transmitted after the blackout.) These blackout data (indicated by a loss of the received power of the telemetry signal at the downrange station) are related to the radio wave cutoff phenomena by the plasma electron density. The vhf antenna is located at a leeward surface of the HYFLEX vehicle (Fig. 5) to avoid the high aerodynamic heating and to keep sending telemetry data.

Plasma Electron and Radio Wave Interference Simulation

Occurrence of a radio wave blackout by plasma electrons can be characterized by plasma frequency f_p , as described in the Introduction. However, the actual phenomena are more complicated because the reflection intensity varies from 0 to 1 as the plasma electron density increases to n_p . Therefore, for the prediction of this gradual change of reflection intensity, it is necessary to calculate the reflection of the radio wave from the plasma layer using a numerical simulation of the interference between the radio wave and plasma electrons. The governing equations for the numerical analysis are the following equations from Maxwell's equations:

$$\frac{\partial \mathbf{E}}{\partial t} = c \nabla \times \mathbf{B} - 4\pi \mathbf{J} \quad (1)$$

$$\frac{\partial \mathbf{B}}{\partial t} = -c \nabla \times \mathbf{E} \quad (2)$$

and the equations of motion for the plasma electrons:

$$\frac{d\mathbf{v}_m}{dt} = \frac{e_m}{m_m} \left(\mathbf{E} + \mathbf{v}_m \times \frac{\mathbf{B}}{c} \right) \quad (3)$$

$$\frac{d\mathbf{x}_m}{dt} = \mathbf{v}_m \quad (4)$$

$$\mathbf{J} = \sum e_m \mathbf{v}_m \delta(\mathbf{x} - \mathbf{x}_m) \quad (5)$$

The influence of ions in the plasma is negligible because the motion of the ions is very small due to their very large mass relative to the electron's mass.

In the discretization, central differences are used for both space and time. Electric field and magnetic field are calculated in space and time alternately. Because the number of actual plasma electrons is very large, the plasma electrons are treated as a superparticle that is a group of plasma electrons. Using the given distribution of plasma electron density calculated by the CFD code, the electric charge of each superparticle is decided at each position. Collisions between the plasma electrons are neglected because the collision frequency is very small compared to the radio wave frequency at this flight condition.

In the discretization of the one-dimensional analysis, E is defined for the z direction, B is defined for the y direction, and the electromagnetic wave is supposed to propagate in the x direction. Moreover, E and B are placed alternately on the grid because E is calculated from B at adjacent grid points on both sides using Eq. (1) and vice versa, where B is calculated from E using Eq. (2). Regarding the plasma electrons, only the z direction velocity of the electrons is produced. The electric current is obtained by the linear interpolation of the plasma particle velocity. These one-dimensional simulation results for the plasma layer of a constant and also step-shaped density distribution were compared with analytical solutions, and very good agreement was shown.¹⁷

In the three-dimensional analysis, it becomes more complicated because the direction of the E and B fields has to be set adequately according to the position. At first, for example, it is assumed that E is defined for the z direction at E_{0z} in Fig. 8. Then the next positions of B are influenced, and the direction of B is for the y direction at the B_{1y} position and for the x direction at B_{1x} . Next E_{2x} and E_{2z} are influenced by B_{1y} and vibrated for the x direction and z direction, respectively. Here both E and B should not be set at the positions of P , Q , R , and S because these positions are not influenced by E_{0z} . Using this grid system, radio wave transmissions can be simulated.

The accuracy of this three-dimensional numerical simulation can be evaluated by comparing its results with those of ground tests of

the reflectometer flight model in which radio waves are reflected by a metallic plate instead of a plasma layer. The results are shown in Fig. 9. The one- and two-dimensional simulation cannot include the correct effect of the distance between the plasma layer and the antenna. This is because the gap should leak the radio waves three dimensionally. The three-dimensional simulation results (which demonstrate the effect precisely in three-dimensional space) agree quite well with the test results. The accuracy of this simulation method is verified by the one-dimensional results for the distributed plasma density and the three-dimensional results for the metal plate in three-dimensional space.

Reflectometer Flight Result and Comparison with the Simulation

The flight data obtained by the reflectometers are shown in Fig. 10. S/N ratios of the reflectometers are -20 dB for 902.85 MHz and -23 dB for 1676.5 MHz, which reveal their performances in detecting small signals from the reflected radio waves. The reflectometer of 902.85 and 1676.5 MHz could detect the signal over 0.1 and 0.07, respectively. Errors, such as noise of telemetry data and temperature drift, are very low and are within only 1 bit, as can be seen by the very small fluctuations of data in Fig. 10. Although this low error level is caused by low resolution (about 0.005, which is not very good, as shown in Fig. 10), the performance of the reflectometer (considering S/N ratio, errors, and resolution) is reasonable for analysis and comparison with the calculated results. For other errors on the reflectometer, there are also effects by the Kevlar window and ceramic tiles between the plasma layer and the antenna, but it has been confirmed by ground tests that these effects can be neglected. The other effects include the change of surface composition of the ceramic tiles by the high aerodynamic heating, i.e., ablation effects, which might occur during the reentry flight. This effect may have shifted the time of the largest radio wave reflection to a later moment because the largest aerodynamic heating happened several seconds after the largest radio wave reflection. However, this effect could be also neglected by considering the relationship of the flight data and CFD results shown later.

The maximum reflection coefficient was about 0.3 at 902.85 MHz and about 0.2 at 1676.5 MHz. The dependency on frequency is qualitatively reasonable because the reflection of the lower frequency should be larger than that of the higher frequency. Regarding the time and duration of blackout, the radio wave reflection occurred during $t = 100 \sim 130$ s, which is consistent with the blackout ($t = 105 \sim 125$ s) observed in the vhf telemetry data.

In Fig. 10, results of the radio wave reflection intensity obtained by the three-dimensional numerical simulations (including real-gas CFD and radio wave and plasma electron interferences, as described earlier) are compared with flight results for 902.85 and 1676.5 MHz. The simulated magnitude of maximum reflection intensity shows good agreement with the flight data. Therefore, this distribution of plasma electron density is a possibility for the actual plasma. In

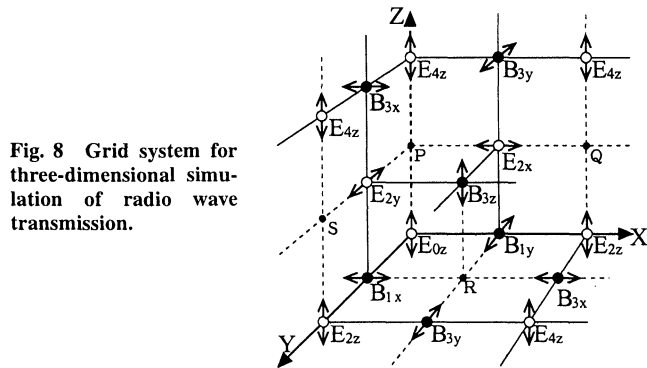
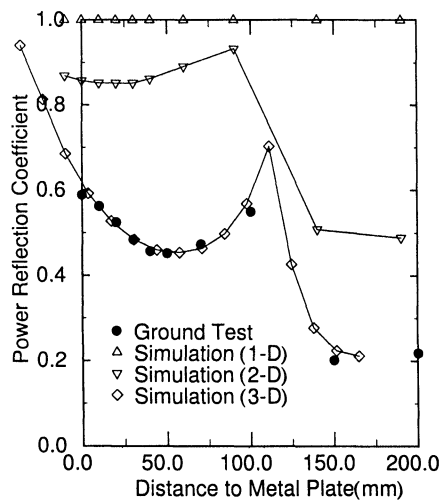
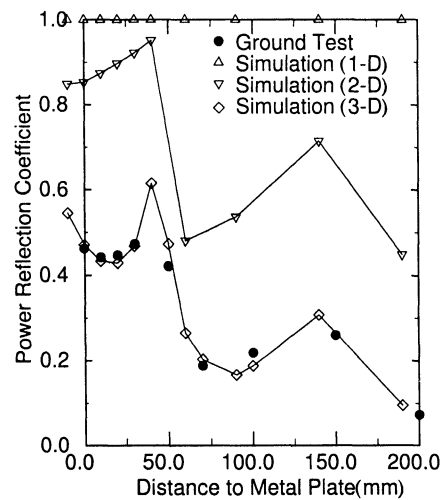


Fig. 8 Grid system for three-dimensional simulation of radio wave transmission.



a) 902.85 MHz



b) 1676.5 MHz

Fig. 9 Calibration results of the reflectometer and calculation by the metallic plate reflection.

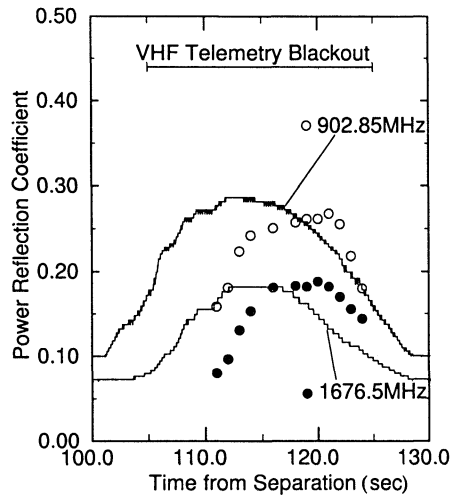


Fig. 10 Flight test results of the reflectometer and comparison with the numerical simulation.

other words, the other distribution could show the same reflection coefficient. Thus, it cannot be concluded that the distribution calculated by CFD is correct by using only the data from the reflectometers. However, as mentioned in the next section, the data of received vhf telemetry intensity show the same kind of good agreement despite the difference in position and magnitude of the density. Thus, the calculated results are reasonable, and it is concluded that the order of maximum plasma electron density is about 10^{11} (particles/cm³) and the thickness of the plasma layer is about 1 cm around the reflectometers, where the thickness is defined by the density that remains over 10% of the maximum density.

However, simulated results show a 5~10-s discrepancy with the flight data in time, especially at the beginning of blackout. This difference of 5 s is not large, but the difference of the reflection coefficient of ≈ 0.1 at 110 s from separation is significant because this value of 0.1 is much larger than the simulation error in Fig. 9. Therefore, this discrepancy warrants examination. This discrepancy is probably not due to any ablation effect because this would shift the discrepancy in Fig. 10 the opposite direction in time.

Although the reason for this discrepancy is not known yet, the CFD model of the real gas may need to be examined more closely using these results. For example, the CFD model might tend to have an error in the much sparser atmosphere. In the future, it will be necessary to check the CFD code to find the reason for this discrepancy by using other flight-test results. Moreover, verification of the CFD results and reflection simulation in a much higher plasma electron condition will be needed because the separation speed of the HYFLEX vehicle was limited to 3.9 km/s. For this purpose, we are again planning measurements in the HOPE-X vehicle, which has a much higher speed than the HYFLEX vehicle, because HOPE-X is a planned reentry from orbit.

VHF Blackout and Comparison with the Simulation

Figure 11 shows the intensity of vhf telemetry radio waves (296.2 MHz) received at the Ogasawara Downrange Station.¹⁶ The vertical axis indicates the strength of the received radio wave that is normalized by the value at 100 s (occurring just before the blackout phenomena). A decrease in intensity (blackout) was detected between $t = 105$ and $t = 125$ s. The value at 100 s is relatively higher than that at 105 and 115 s, but it is considered reasonable because the trend of the intensity would show an increase if the blackout phenomena did not occur. This trend of an increase occurred because the vehicle was getting closer to the Ogasawara Downrange Station. After 130 s, the intensity became very high because the vehicle was getting closer and skyline interference occurred, which was the effect of reflection and diffraction by the mountains.

Here the numerical simulation results using one-dimensional analysis are shown. A three-dimensional calculation is not necessary for this analysis because the radio waves reach the Ogasawara

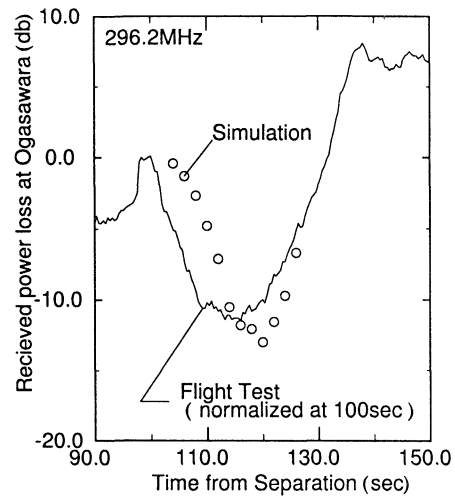


Fig. 11 Intensity of vhf telemetry radio waves (296.2 MHz) received at the Ogasawara Downrange Station and comparison with the numerical simulation.

Downrange Station directly and the reflected waves in other directions are considered negligible. The calculated results show good agreement, except that the minimum point is shifted by 5~10 s in time. As mentioned in the reflectometer results, the plasma distributions calculated by CFD are considered to be reasonable; the maximum density is about $2\sim 3 \times 10^9$ (particle/cm³), and the thickness of the plasma layer is about 50~60 cm.

This discrepancy in time is the same for the reflectometer results. However, the flow condition around the vhf antenna, which was at the leeward side of the vehicle, is very different from the flow condition around the reflectometer, which was at the windward side. Thus, the aerodynamic heating is weak, and the density and pressure are small. Also, the measurement procedures are different for the reflected waves that were measured by the reflectometer and the transmitted waves that were measured by the vhf telemetry. Moreover, the simulations of radio wave and plasma electron interference are different. That is, one- and three-dimensional simulations were applied. However, these two relationships between simulations and flight tests showed the same discrepancy. The results are very interesting, and these measurement systems and the interference simulation are considered to have sufficient accuracy. The procedure is able to verify results from the real-gas CFD code, and these results give clues for the improvement of the real-gas model used in the CFD calculation.

Conclusions

In the HYFLEX, measurements by reflectometer and detection of vhf blackout phenomena were conducted, and their results were compared with the calculated results using real-gas CFD and numerical simulation between radio waves and plasma electrons. The plasma layer was predicted by the CFD. The thickness of the plasma layer around the reflectometer was about 1 cm, and the order of the highest density was about 10^{11} (particles/cm³) after 120 s from separation. Also, the plasma density was calculated near the vhf telemetry antenna by CFD, the peak density was about 3×10^9 (particles/cm³), and the thickness was about 50 cm.

Using these CFD results, radio wave and plasma electron interference simulations were conducted to predict reflection coefficients from the reflectometer and the intensity received at the ground station. Calculated results of the maximum reflection coefficients and the minimum received intensity showed good agreement with flight-test results. Presently, the obtained time discrepancy in the occurrence of the peak plasma electron density, which was observed in comparison of both the reflectometer data and the ground station data in a very similar manner, gives a clue for the improvement of the real-gas model used in the CFD calculations.

Acknowledgments

The authors wish to thank M. Shirouzu of the National Aerospace Laboratory, M. Yamamoto of the National Space Development

Agency, and all other members involved in the HYFLEX project for contributing some useful information and for their kind suggestions and encouragement.

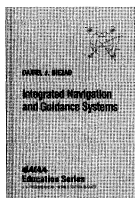
References

- ¹Shirouzu, M., and Yamamoto, M., "Overview of the HYFLEX Project," AIAA Paper 96-4524, Nov. 1996.
- ²Sakurai, H., Kobayashi, M., Yamazaki, I., Shirouzu, M., and Yamamoto, M., "Development of the Hypersonic Flight Experimental Vehicle," *47th International Astronautical Congress*, International Astronautical Federation, IAF Paper 96-V.2.07, Oct. 1996.
- ³Watanabe, S., Ishimoto, S., and Yamamoto, Y., "Aerodynamic Characteristics Evaluation of Hypersonic Flight Experiment (HYFLEX) Vehicle Based on Flight Data," AIAA Paper 96-4527, Nov. 1996.
- ⁴Kai, T., and Ohtake, K., "Thermal Protection System Evaluation of the HYFLEX Vehicle," AIAA Paper 96-4526, Nov. 1996.
- ⁵Ishimoto, S., Takizawa, M., Suzuki, H., and Morito, T., "Flight Control System of Hypersonic Flight Experiment Vehicle," AIAA Paper 96-3403, July 1996.
- ⁶Suzuki, H., Ishimoto, S., and Morito, T., "Postflight Evaluation of the HYFLEX Guidance, Navigation, and Control," AIAA Paper 96-4525, Nov. 1996.
- ⁷Inouye, Y., Fujii, K., Takizawa, M., Takaki, R., Watanabe, S., and Ito, T., "Flight Results of HYFLEX Onboard Measurements," AIAA Paper 96-4528, Nov. 1996.
- ⁸Takaki, R., and Takizawa, M., "ADS Measurement of HYFLEX (Hypersonic Flight Experiment)," AIAA Paper 97-0193, Jan. 1997.
- ⁹Watanabe, S., and Takaki, R., "RCS Gas-Jet Interaction in the Hypersonic Flight Experiment, HYFLEX," AIAA Paper 97-0524, Jan. 1997.
- ¹⁰Woods, W. C., Arrington, J. P., and Hamilton, H. H., II, "A Review of Preflight Estimates of Real Gas Effects on Space Shuttle Aerodynamic Characteristics, Shuttle Performance: Lessons Learned, Part 1," NASA CP-2283, Oct. 1983, pp. 309-346.
- ¹¹Brauckmann, G. J., Paulson, J. W., Jr., and Weilmuenster, K. J., "Experimental and Computational Analysis of the Space Shuttle Orbiter Hypersonic 'Pitch-Up Anomaly,'" AIAA Paper 94-0632, Jan. 1994.
- ¹²Takaki, R., and Ito, T., "CFD Analysis for Hypersonic Flight Experiment (HYFLEX)," *Proceedings of the 14th NAL Symposium on Aircraft Computational Aerodynamics*, National Aerospace Lab., NAL-SP-34, Tokyo, Japan, 1997, pp. 49-54 (in Japanese).
- ¹³Takaki, R., and Yamamoto, Y., "Numerical Analysis of Three-Dimensional Hypersonic Non-Equilibrium Flows Around Re-Entry Vehicles," *Proceedings of the 15th NAL Symposium on Aircraft Computational Aerodynamics*, National Aerospace Lab., NAL-SP-37, Tokyo, Japan, 1998, pp. 121-126 (in Japanese).
- ¹⁴Takaki, R., "Hypersonic CFD High Enthalpy Flow—Numerical Simulation by Parallel Computer," *Proceedings of First U.S.-Japan Symposium on High Speed Ground Testing and Computations*, Univ. of Tennessee Space Inst., Tullahoma, TN, 1997.
- ¹⁵Kurotaki, T., "Effects of Wall Catalysis on the Non-Equilibrium Hypersonic Flow Around Reentry Vehicle," *Proceedings of the 14th NAL Symposium on Aircraft Computational Aerodynamics*, National Aerospace Lab., NAL-SP-34, Tokyo, Japan, 1997, pp. 77-82 (in Japanese).
- ¹⁶Teraoka, K., and Morito, T., "Development of Electrical Components and Evaluation of Bus System," *Proceedings of the 14th NAL Symposium on Aircraft Computational Aerodynamics*, National Aerospace Lab., NAL-SP-32, Tokyo, Japan, 1996, pp. 88-102 (in Japanese).
- ¹⁷Ito, T., Takaki, R., and Teraoka, K., "Plasma Density Measurement on HYFLEX Vehicle," *Proceedings of 37th Space Sciences and Technology Conference of JSASS*, Japan Society for Aeronautical and Space Sciences, Tokyo, Japan, 1993, pp. 247, 248 (in Japanese).

I. D. Boyd
Associate Editor

Integrated Navigation and Guidance Systems

Daniel J. Biezad, California Polytechnic State University, San Luis Obispo



Includes software!

AIAA Education Series
1999, 235 pp Hardcover
ISBN 1-56347-291-0
List Price: \$79.95
AIAA Member Price: \$54.95
Source: 945

Beginning with the basic principles of navigation, this book takes a step beyond introductions with a concise look at the flight applications of inertial navigation systems integrated with Global Positioning System (GPS). Written at the senior engineering college level, the textbook takes a tutorial approach, weaving interrelated disciplines together with interactive computer exercises and AINSBOOK software for error analysis and Kalman filter simulation. It looks at traditional navigation radio aids, inertial guidance systems, and Kalman filters, and GPS applications in navigation, precision approach and landing, attitude control, and air traffic control. More than 100 figures, photos, and tables add to the textbook's value.

Contents:

Navigation over Earth's Surface • Newton's Laws Applied to Navigation • Inertial Navigation Sensors and Systems • Concept of Uncertainty in Navigation • Kalman Filter Inertial Navigation System Flight Applications • Global Positioning System • High Accuracy Navigation Using Global Positioning System • Differential and Carrier Tracking Global Position System Applications • Flight Testing Navigation Systems • Navigation Computer Simulations • Appendix A: Abbreviations and Acronyms • Appendix B: Discussion Questions for Integrated Navigation and Guidance Systems • Appendix C: Web Sites by Chapter • References • Index



American Institute of Aeronautics and Astronautics

Publications Customer Service, 9 Jay Gould Ct., P.O. Box 753, Waldorf, MD 20604
 Fax 301/843-0159 Phone 800/682-2422 E-mail aiaa@tascot1.com
 8 am-5 pm Eastern Standard Time

CA and VA residents add applicable sales tax. For shipping and handling add \$4.75 for 1-4 books (call for rates for higher quantities). All individual orders—including U.S., Canadian, and foreign—must be prepaid by personal or company check, traveler's check, international money order, or credit card (VISA, MasterCard, American Express, or Diners Club). All checks must be made payable to AIAA in U.S. dollars, drawn on a U.S. bank. Orders from libraries, corporations, government agencies, and university and college bookstores must be accompanied by an authorized purchase order. All other bookstore orders must be prepaid. Please allow 4 weeks for delivery. Prices are subject to change without notice. Returns in sellable condition will be accepted within 30 days. Sorry, we cannot accept returns of case studies, conference proceedings, sale items, or software (unless defective). Non-U.S. residents are responsible for payment of any taxes required by their government.